Separation Science and Technology
Publication details, including instructions for authors and subscription information:
http://www.informaworld.com/smpp/title~content=t713708471

Chromatographic Analysis of Limonene and Linalool on Silica Gel in Supercritical Carbon Dioxide

Masaki Sato; Motonobu Goto; Akio Kodama; Tsutomu Hirose

To cite this Article Sato, Masaki , Goto, Motonobu , Kodama, Akio and Hirose, Tsutomu(1998) 'Chromatographic Analysis of Limonene and Linalool on Silica Gel in Supercritical Carbon Dioxide', Separation Science and Technology, 33: 9, 1283 — 1301
To link to this Article: DOI: 10.1080/01496399808544984
URL: http://dx.doi.org/10.1080/01496399808544984

SEPARATION SCIENCE AND TECHNOLOGY, 33(9), pp. 1283–1301, 1998

Chromatographic Analysis of Limonene and Linalool on Silica Gel in Supercritical Carbon Dioxide

MASAKI SATO, MOTONOBU GOTO,* AKIO KODAMA, and TSUTOMU HIROSE
DEPARTMENT OF APPLIED CHEMISTRY AND BIOCHEMISTRY
KUMAMOTO UNIVERSITY
KUMAMOTO 860, JAPAN

ABSTRACT

Adsorption behavior of limonene and linalool, which are respectively the principal constituents of terpene and oxygenated compounds in citrus oil, on silica gel in the presence of supercritical carbon dioxide was analyzed by the tracer response method. In this study a two-column system was used to eliminate the effect of nonideal behavior at the sample injection. Adsorption equilibria and mass transport properties were evaluated by means of the moment method at pressures of 8.8–23.5 MPa and temperatures of 313–333 K. The adsorption equilibrium constant was larger for higher temperature and lower pressure when linalool was selectively adsorbed on silica gel. The apparent heat of adsorption ranged from −20 to 230 kJ/mol. The Peclet number and the ratio of intraparticle effective diffusivity to molecular diffusivity were 0.013–0.257 and 0.002–0.716, respectively.

Key Words. Supercritical fluid; Moment method; Adsorption equilibrium constant; Mass transfer; Citrus oil

INTRODUCTION

The supercritical fluid extraction process has received increasing attention in the chemical, food, perfume, and pharmaceutical industries. Carbon dioxide

* To whom correspondence should be addressed. FAX: +81-96-342-3679. E-MAIL: mgoto@kumamoto-u.ac.jp

is suitable as a solvent for the isolation of valuable substances from natural matrices because of its low critical temperature, no residual problem, and harmless properties. Decaffeination of coffee beans is a commercial example of the separation of undesirable and desirable substances. In this case, high selectivity can be achieved. Unfortunately, in many cases the selectivity in supercritical fluid extraction is relatively low. The decaffeination process of coffee beans is an exceptional case where high selectivity was achieved owing to the roasting process. It is desired to separate more selectively to increase the value of natural products.

To achieve high selectivity, extensive research and development has been done in the last decade involving fractionation towers and chromatography. Introduction of adsorbents into a supercritical fluid extraction system is one of the most attractive methods as in supercritical fluid chromatography. Thermodynamic and kinetic studies of adsorption systems in the presence of supercritical fluid are important in the design of adsorptive separation processes. Tan and Liou (1–3) analyzed the desorption behavior of organics from activated carbon by an irreversible first-order kinetic model. Recasens et al. (4) developed a general mathematical model including axial dispersion, external and intraparticle mass transfer, and nonlinear adsorption–desorption kinetics. Srinivasan et al. (5) applied a first-order reversible adsorption model to the desorption of ethyl acetate from activated carbon. Erkey and Akgerman (6), Lee et al. (7, 8), and Goto et al. (9) applied an impulse response technique to determine the adsorption equilibria and rates in supercritical carbon dioxide (SC-CO_2). On the other hand, Iwai et al. (10), Madras et al. (11), and Macnaughton and Foster (12) applied a step response technique to determine the adsorption equilibria.

Fractionation of citrus oil is an important subject in the perfume and food industries. Citrus oil predominantly consists of terpenes and oxygenated compounds. Terpenes are removed to stabilize and concentrate the flavor products. Although terpenes have been conventionally removed by distillation, the distillation process thermally degrades citrus oil. Supercritical fluid extraction processes have been investigated to remove terpenes from citrus oil. Coppella and Barton (13), Stahl and Gerard (14), and Yamauchi and Saito (15) studied the preparation of lemon oil, and Temelli et al. (16) studied the extraction of orange oil. However, simple extraction was not successful since it is difficult to find the optimal balance between solubility and selectivity. That is, a lower pressure gave a higher selectivity but a lower extraction yield, whereas a higher pressure gave a higher yield but a lower selectivity.

Yamauchi and Saito (15) studied the fractionation of lemon oil by supercritical fluid chromatography. They used silica gel as an adsorbent and fractionated lemon oil into three fractions. They could obtain the terpene-rich fraction at 10 MPa, the ester-rich fraction at 20 MPa, and the alcohol- and aldehyde-

rich fractions at 20 MPa with ethanol as the entrainer. Their result shows oxygenated compounds could be selectively adsorbed on silica gel in supercritical carbon dioxide. Barth et al. (17) also reported the deterpenation process of lemon peel oil by desorption from a silica gel. By charging the feed directly to a silica gel bed followed by desorption at a CO_2 density of 400 kg/m^3, they successfully concentrated the oxygenated compounds from 3.4 to 76%. Chouchi et al. (18) also studied the fractionation of various citrus oil with silica gel and obtained 2–50 times the amount of enriched oxygenated compounds by desorption of solutes with SC-CO_2 at 313 K and 25 MPa.

In order to design the adsorption process, it is essential to understand the thermodynamic and kinetic properties. Our objective is to obtain the adsorption equilibrium constant, effective diffusivity, and axial dispersion by moment analysis of tracer response for the design of fractionation processes for citrus oil. Used as adsorbates were limonene and linalool, which are the principal constituents of terpenes and oxygenated compounds in orange oil, respectively. Three types of silica gel were used as the adsorbent. The dynamic properties were measured for the system of limonene/silica gel/CO_2 and linalool/silica gel/CO_2.

EXPERIMENTAL

A schematic diagram of the experimental apparatus is shown in Fig. 1. Carbon dioxide from a cylinder with a siphon attachment (Uchimura Sanso Ltd.) was passed through a cooled line and compressed to operating pressure by a high pressure pump. The compressed CO_2 was passed through a line immersed in an ethanol bath in order to reach the desired temperature, and through an injector, pre-column, adsorption column, and UV detector (Jasco, UV-970). The pressure in the system was controlled by the backpressure

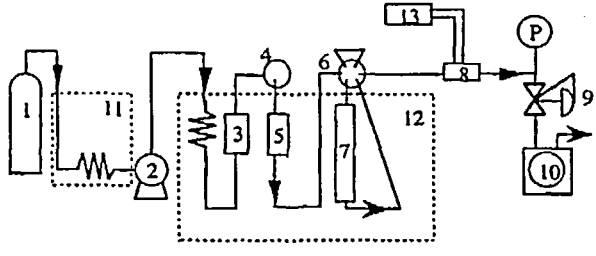

FIG. 1 Experimental apparatus. (1) CO_2 cylinder, (2) high pressure pump, (3) drying column, (4) injector, (5) pre-column, (6) 6-port valve, (7) adsorption column, (8) UV detector, (9) backpressure regulator, (10) dry test meter, (11) cooling bath, (12) ethanol bath, (13) computer.

regulator (Tescom Inc.) and monitored at the pump and after the UV detector. In this work the pressure drop between the pump and the detector was up to 2.0 MPa. The pressure values at the UV detector, that is, at the exit of the column, were used as an operating pressure. The CO_2 flow rate was regulated by the high pressure pump and monitored with a dry gas meter.

The sample used was liquid; 1 μL pulse of sample was injected into the supercritical fluid phase from the injection valve with a microcylinder. This method has a problem when the liquid phase sample does not easily dissolve in the supercritical fluid phase. As will be discussed later, this is the case for our supercritical fluid system. To solve this problem we developed a two-column system consisting of a pre-column and an adsorption column in series. The pre-column acts as dissolver of sample solute into supercritical fluid. Completely dissolved solute in the pre-column flows into the adsorption column. The output signal of the pre-column, which is equivalent to the input of the adsorption, and the output signal of the adsorption column were monitored continuously. The same type of silica gel was packed into both the pre-column and the adsorption column. Either an input signal or output signal of the adsorption column was obtained by switching a 6-port valve. Therefore, the actual behavior of the adsorption column could be evaluated by subtracting the input signal from the output signal.

Three types of silica gel normally used for liquid chromatography (SG-1), gas chromatography (SG-2), and HPLC (SG-3) were used as adsorbents. The properties of the packed columns are given in Table 1. *d*-Limonene and linalool (Kanto Chem. Ltd.) were used as adsorbates, and CO_2 was used as the mobile phase.

TABLE 1
Properties of the Adsorption Column

	SG-1[a]	SG-2[b]	SG-3[c]
Pre-column length (m)	0.05	0.05	0.05
Pre-column diameter (m)	0.0076	0.0076	0.0076
Column length (m)	0.25	0.05	0.05
Column diameter (m)	0.0076	0.0068	0.0068
Bed porosity (—)	0.30	0.40	0.40
Particle radius (μm)	94	82	25
Particle porosity (—)	0.74	0.41	0.80
Particle density (kg/m^3)	2200	1900	4400

[a] SG-1: Silica gel 120 (Nacalai Tesque Inc.).
[b] SG-2: Silica gel 80/100 (GL Science).
[c] SG-3: Wakogel LC-50H (Wako Pure Chem. Ind. Ltd.).

MOMENT ANALYSIS

The most common method to obtain the equilibrium and the transport properties from chromatographic elution curves in the infinite dilution region is the moment method suggested by Kubin (19). This method can evaluate the thermodynamic and transport parameters by comparing an experimental elution curve with a mathematical model of the system. The general approach for the moment method was summarized by Suzuki (20) and Ruthven (21). The first absolute moment and the second central moment of the chromatographic elution curve are calculated by

$$\mu_1' = \int_0^\infty Ct\, dt \Big/ \int_0^\infty C\, dt \tag{1}$$

$$\mu_2 = \int_0^\infty C(t - \mu_1')^2\, dt \Big/ \int_0^\infty C\, dt \tag{2}$$

These moments can be directly calculated from the absorbance of the UV detector without conversion to the concentration in our system since the Beer–Lambert relation holds. The governing equations for a fixed bed of adsorbent particles were given by Kubin (19), accounting for the adsorption equilibrium coefficient, axial dispersion, external film mass transfer, intraparticle diffusion, and adsorption rate. The moment expressions obtained from the analytical solution in the Laplace domain are given by

$$\mu_1' = \frac{Z}{v}(1 + \delta_0) + \mu_{1(\text{input})}' \tag{3}$$

$$\mu_2 = \frac{2Z}{v}(\delta_{ax} + \delta_f + \delta_d + \delta_{ad}) + \mu_{2(\text{input})} \tag{4}$$

where

$$\delta_0 = \frac{1 - \epsilon}{\epsilon}(\epsilon_p + K_A) \tag{5}$$

$$\delta_{ax} = \frac{E}{v^2}(1 + \delta_0)^2 \tag{6}$$

$$\delta_f = \frac{1 - \epsilon}{\epsilon}\frac{R}{3k_f}(\epsilon_p + K_A)^2 \tag{7}$$

$$\delta_d = \frac{1 - \epsilon}{\epsilon} \frac{R^2}{15D_e} (\epsilon_p + K_A)^2 \quad (8)$$

$$\delta_{ad} = \frac{1 - \epsilon}{\epsilon} \frac{K_A^2}{k_a} \quad (9)$$

In the following analysis the adsorption rate constant, k_a, was assumed to be infinitely large because the adsorption rate is usually larger than the mass transfer rate in chromatographic processes. The external mass transfer coefficient, k_f, was estimated by the Wakao–Kaguei correlation (22).

RESULTS AND DISCUSSION

Significance of Two-Column System

In this work the two-column system was employed for chromatographic analysis to eliminate the effect of nonideal behavior at the sample injection port. We discuss the importance of the two-column system in comparison with the normal one-column system.

Figure 2 shows the first moment, μ_1, plotted versus the inert fluid retention time, Z/v, for the pre-column packed with SG-1 on the assumption of an ideal

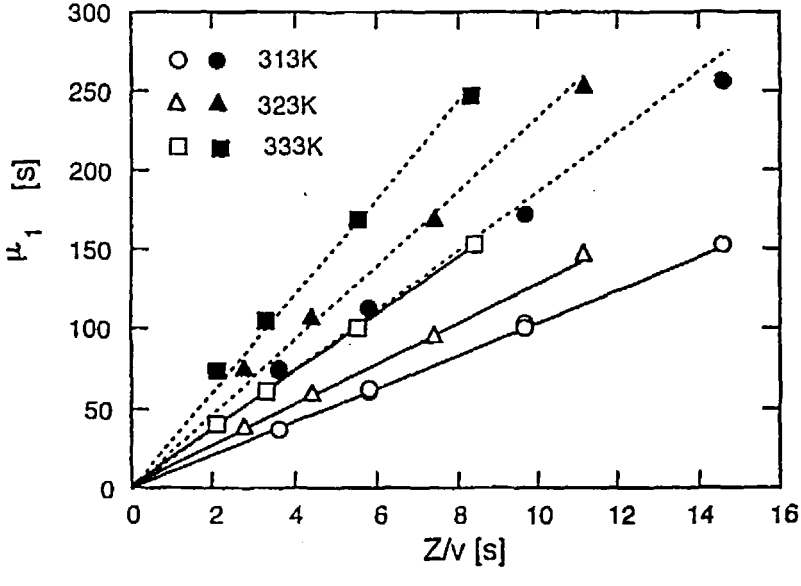

FIG. 2 Variation of the first moment with Z/v for the pre-column at 11.8 MPa for SG-1. Open symbols: limonene; filled symbols, linalool.

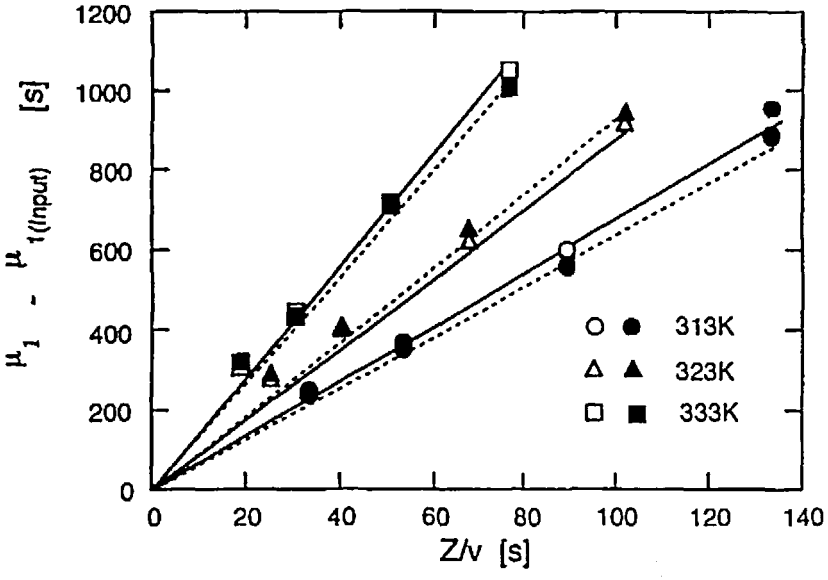

FIG. 3 Variation of the first moment with Z/v for the adsorption column at 11.8 MPa for SG-1. Open symbols: limonene; filled symbols, linalool.

input pulse. The slope of the regression line between limonene and linalool at each temperature was different, indicating that two components were chromatographically separated. Figure 3 shows the first moment, $\mu_1' - \mu_{1(input)}'$, for the adsorption column of SG-1 with correction of the input peak. The straight lines in Fig. 3 indicate that two components were not separated. Since the same adsorbent was packed in both the pre-column and the adsorption column, the results obtained from Figs. 2 and 3 should be the same. This contradiction is explained in the following discussion.

At the inlet of the pre-column, the injected sample flows into the pre-column as a liquid phase. When dissolving of the liquid solute into the supercritical fluid is slow or inadequate heat of solution is provided, a part of the solute may be adsorbed onto the adsorbent directly from the liquid phase. Once the solute is adsorbed, the solute is later desorbed into the supercritical fluid. Thus, the phenomena observed at the exit of the pre-column must be complicated when the chromatographic behavior is influenced by equilibria for supercritical fluid/solid, liquid/solid, and supercritical fluid/liquid, and by kinetics of slow dissolving of solute into the supercritical fluid.

Additional evidence of these phenomena is given by UV spectrum measurement. The UV spectrum was measured at several points on the response peaks.

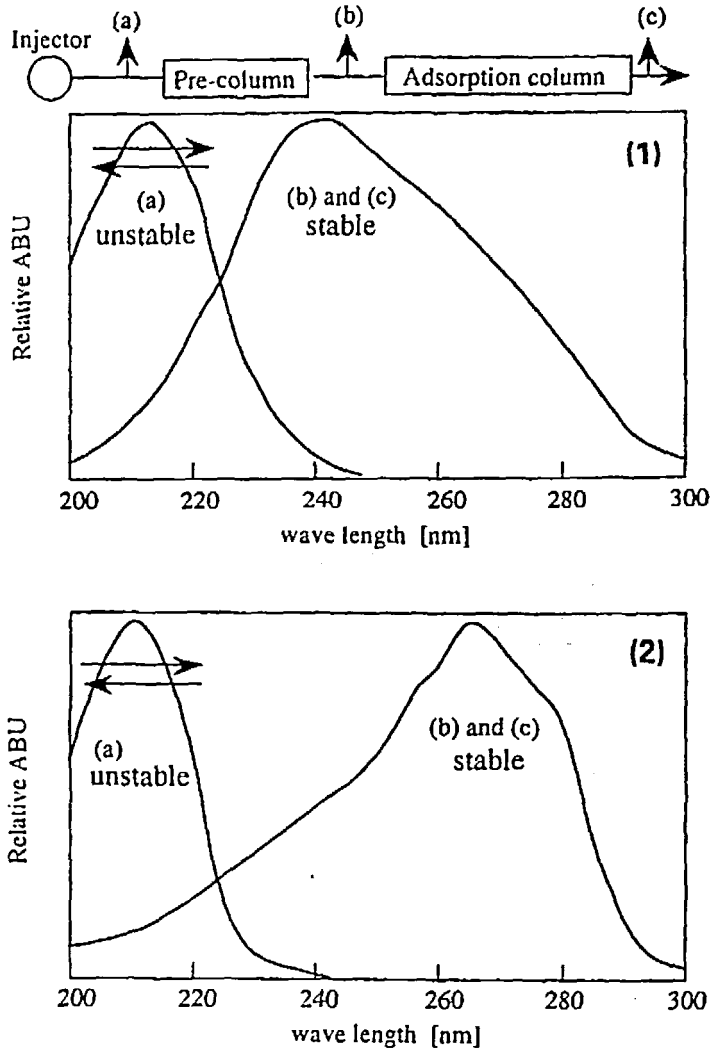

FIG. 4 UV spectra of limonene (1) and linalool (2) in SC-CO_2 detected at the points shown.

Figure 4 shows the UV spectrum of limonene (Fig. 4-1) and linalool (Fig. 4-2) in the presence of SC-CO_2 measured at three points: just after the injector (a), after the pre-column (b), and after the adsorption column (c). For both limonene and linalool, the spectrum measured at (a) is obviously different from those at (b) and (c), indicating that the state of the solute is different.

The spectrum at (a) was unstable, that is, it fluctuated with time, while the spectrum at (b) or (c) was stable and had maximum absorbance at 240 nm for limonene or at 265 nm for linalool. It is expected that the solute at (a) exists partially as a liquid, whereas the solute at (b) and (c) is completely dissolved in SC-CO_2. Thus, the pre-column plays a role in dissolving the solute completely into the supercritical fluid. Without using the pre-column, the solute introduced at the injector could not be dissolved completely into the supercritical fluid due to the slow dissolving rate. Other attempts to dissolve the solute in supercritical carbon dioxide, such as using a glass beads packing and heating the injector, were carried out. However, the problem could not be solved.

Thus the phenomena observed for the pre-column is not simply a supercritical fluid/solid system. A simple chromatographic system that consists of an injector and a single column cannot give accurate information for such a system. Therefore, to determine the pure phenomena for the supercritical fluid/solid system it should be measured with a two-column system.

Using a pre-saturator to dissolve the solute (6–8) is an alternative, simple method to analyze the adsorption equilibrium in a supercritical fluid. However, the injection method by a microcylinder used for GC or HPLC is more popular and useful for chromatographic analysis. We discuss the problem, the importance of the procedure, and analysis with a microcylinder injection.

First Moment Analysis

For a linear adsorption isotherm system, the first absolute moment characterizes the retention time of the peak of the response curve and gives information concerning the adsorption equilibrium constant. The adsorption equilibrium constant can be calculated from the slope of the straight line in the plot of the first moment versus the retention time of an inert fluid through the column, Z/v.

Adsorption equilibrium constants, K_A, calculated for the adsorption column are presented in Table 2. Differences in K_A between limonene and linalool were largest for SG-3 where linalool was selectively adsorbed on the silica gel. K_A increased with a decrease in pressure or an increase in temperature for all types of silica gel. The temperature and pressure dependencies of the adsorption equilibrium constant in a supercritical fluid were different from those in gas and liquid.

Retrograde Phenomena

Many investigators (5, 6, 14–16) have reported the retrograde phenomena in the vicinity of the critical point where the dependency of the solubility and the adsorption equilibrium constant is different from the usual liquid- or

TABLE 2
Adsorption Equilibrium Constants

Conditions			K_A (—)					
			SG-1		SG-2		SG-3	
Temperature (K)	Pressure (MPa)	Density (kg/m^3)	Limonene	Linalool	Limonene	Linalool	Limonene	Linalool
313	8.8	481	3.28	3.41				
313	11.8	710	1.43	1.39	2.51	4.35	1.10	53.46
313	14.7	773	1.26	1.41			0.92	44.24
313	17.7	815	1.32	1.11			0.92	27.94
313	23.5	871					0.79	31.19
323	8.8	269	10.81	11.20				
323	11.8	576	2.41	2.54	4.94	6.16	2.41	88.04
323	14.7	689	1.45	1.56			1.36	55.19
323	17.7	750					0.92	35.08
323	23.5	822					0.74	27.02
333	11.8	420	4.30	4.14	6.50	9.18	5.52	319.3
333	14.7	591	2.54	3.06			1.75	77.09
333	17.7	678	1.76	1.80			1.10	36.62
333	23.5	770					0.66	26.10

gas-phase phenomena. One attribution for the retrograde phenomena was observed in supercritical fluid chromatography and was discussed by Kelley and Chimowitz (24).

For a linear adsorption system, chromatographic impulse response analysis supplies an important thermodynamic property involving the adsorption equilibrium constant and the capacity factor. They are characterized by the retention time of the peak of the response curve and have the following relationship with the porosity of the bed and adsorbent particles.

$$k = \frac{t_i - t_0}{t_0} = \frac{(1 - \epsilon)K_A}{\epsilon + (1 - \epsilon)\epsilon_p} \tag{10}$$

The relation between capacity factor and temperature at constant pressure is expressed by equating the fugacities in the supercritical phase and the solid phase (24):

$$\left(\frac{\partial \ln k}{\partial T}\right)_P = \left(\frac{(h_i^0 - h_i^m) - (h_i^0 - h_i^s)}{R_g T^2}\right) + \alpha_m \tag{11}$$

where α_m is the volume expansivity and the superscripts 0, m, and s represent the ideal gas phase, mobile phase, and solid phase, respectively. The capacity

factor increases with temperature when the following inequality is satisfied:

$$(h_i^0 - h_i^m) > (h_i^0 - h_i^s) \quad (12)$$

This inequality is always satisfied in the retrograde region, and hence the adsorption equilibrium constant increases with temperature. Thus, in adsorption in the vicinity of the critical point, the partial molar enthalpy of the solute in a supercritical fluid may have a more significant effect than the heat of adsorption. The analogous relation to Eq. (11) is the van't Hoff equation, where the apparent heat of adsorption, ΔH_{app}, corresponds to $(h_i^0 - h_i^m) > (h_i^0 - h_i^s)$.

The apparent heat of adsorption, ΔH_{app}, was estimated from the slope of the fitted line in the van't Hoff plot where $\ln(K_A)$ was plotted against $1/T$. The obtained values of ΔH_{app} are shown in Table 3. The values obtained in this work ranged from -20 to 230 kJ/mol. In the vicinity of critical pressure, adsorption of solutes induced endothermic behavior ($\Delta H_{app} > 0$) and the apparent heat of adsorption decreased with an increase in pressure. These positive values indicate that the inequality in Eq. (12) is satisfied. However, at higher pressure, far from critical point (23.5 MPa), exothermic behavior ($\Delta H_{app} < 0$) was observed. This result shows that the adsorption equilibrium constant decreases with increasing temperature. Consequently, the physical properties of a supercritical fluid approach liquid properties with an increase in pressure.

Another interesting property in supercritical fluid chromatography is the solute partial molar volume. The partial molar volume is a fundamental property of solution for probing molecular interaction at infinite dilution in the supercritical fluid. A very large negative partial molar volume has been observed in the vicinity of the critical point, which is evidence of the clustering phenomena (26). That is, in the vicinity of the critical point, solvent molecules condense around the solute, resulting in a much greater local density than

TABLE 3
Apparent Heat of Adsorption

Pressure (MPa)	ΔH_{app} (kJ/mol)					
	SG-1		SG-2		SG-3	
	Limonene	Linalool	Limonene	Linalool	Limonene	Linalool
8.8	231	230				
11.8	110	109	95.4	74.3	161	177
14.7	69.6	76.7			59.7	54.9
17.7	28.3	48.6			22.1	20.3
23.5					−18.1	−17.8

the bulk density of the fluid. The clustering is related to solute–solvent interaction and affects such macroscopic properties as solubility and adsorption equilibria. This property is also related to the temperature and pressure dependency of the capacity factors in supercritical fluid chromatography. The thermodynamic approach of solute retention has been developed by various investigators [e.g., Chimowitz and Kelley (23, 24), Shim and Johnston (25), and Yonker et al. (27)].

Chimowitz and Kelley (23) gave the relationship between the density dependence of the capacity factor at constant temperature to the partial molar volume of the solute in the infinite dilution region as

$$\left(\frac{\partial \ln k}{\partial \ln \rho}\right) = -\left(1 - \frac{V_i^{m\infty}}{R_g T K_T}\right) \tag{13}$$

where K_T is the isothermal compressibility. The above equation holds in the infinite dilution region and at large negative partial molar volume. Kumar and Johnston (28) gave experimental evidence that $V_i^{m\infty}/K_T$ is independent of density in the vicinity of the critical point. Consequently, when the plot of $\ln(k)$ versus $\ln(\rho)$ is linear, the partial molar volume of solute at infinite dilution can be calculated by Eq. (13).

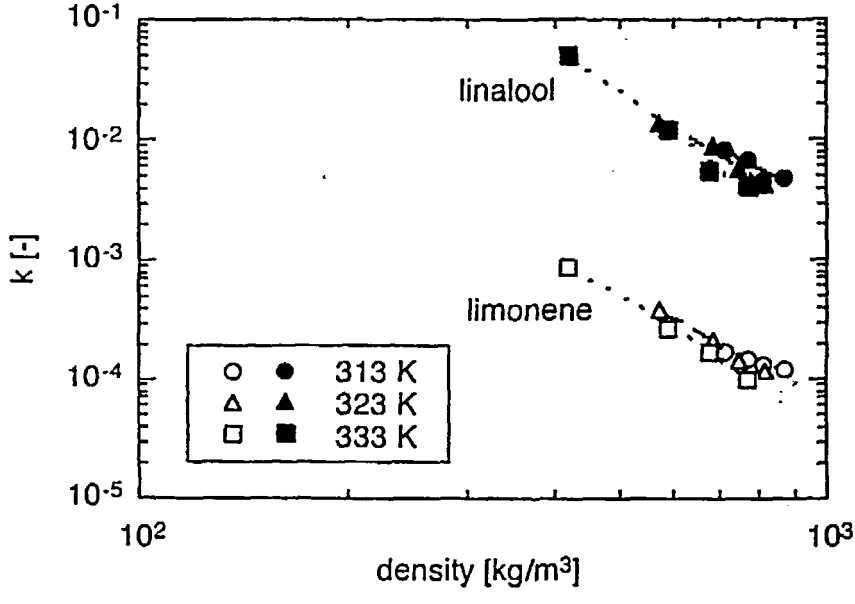

FIG. 5 Variation of capacity factor with density for SG-3.

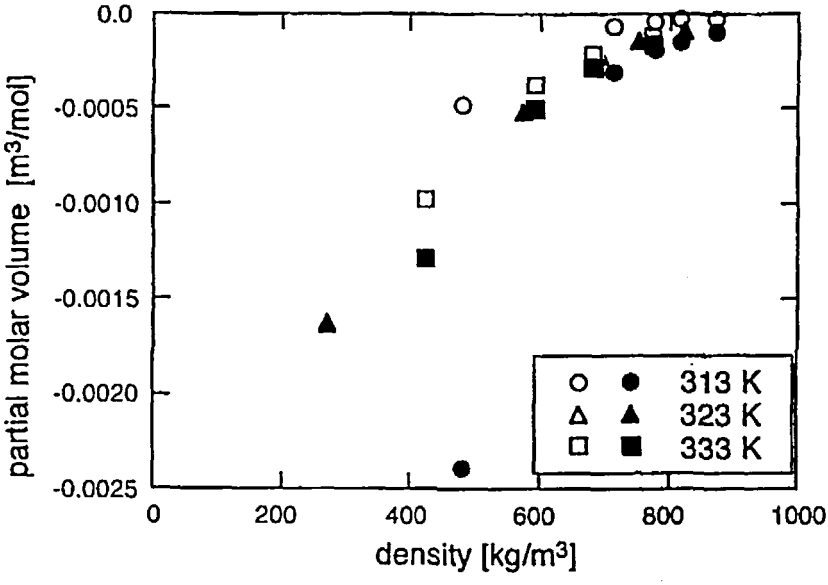

FIG. 6 Partial molar volumes of limonene and linalool at infinite dilution in SC-CO_2 for SG-3. Open symbols: limonene; filled symbols, linalool.

The capacity factors were correlated linearly in log-log coordinates as a function of solvent density as shown in Fig. 5 for SG-3. The capacity factor lay well on a straight line for each temperature. Figure 6 shows the partial molar volume at infinite dilution, obtained from Eq. (13), as a function of density. Isothermal compressibility was calculated from the Peng–Robinson equation of state (29) with densities obtained from IUPAC tables (30). The results in Fig. 6 indicate a large negative partial molar volume in the present experimental conditions. The solute partial molar volume decreases as the condition of the system approaches the critical point, and these values are in good agreement with those for the ethyl acetate/activated carbon/SC-CO_2 system (31), the naphthalene/alumina/SC-CO_2 system (6) and the naphthalene/C18/SC-CO_2 and phenanthrene/C18/SC-CO_2 systems (25). The partial molar volume is smaller for limonene than for linalool due to its larger polarity or stronger solute–solvent interaction. The results are also supported by the observation of the solubility equilibrium in supercritical fluid systems. Consequently, the temperature and pressure dependency of the adsorption equilibrium constant in the vicinity of the critical point, discussed above, and which is a phenomenon contrary to the gas and liquid phases, is explained by the large solute–solvent intermolecular interaction in the near-critical region.

Second Moment Analysis

The second central moment characterizes the width of the peak of the response curve and gives information concerning mass transport properties. Equation (4) was rearranged to

$$\frac{\mu_2 - \mu_{2(\text{input})}}{2(\mu_1' - \mu_{1(\text{input})}')} = \frac{E}{v^2}(1 + \delta_0) + \frac{\delta_1}{(1 + \delta_0)} \tag{14}$$

where

$$\delta_1 = \delta_{ad} + \delta_f + \delta_d \tag{15}$$

Since E/v can be considered to be constant at low Reynolds number in a packed bed, a plot of the left-hand side of Eq. (14) against $1/v$, as shown in Fig. 7, gives a straight line with an intercept of $\delta_1/(1 + \delta_0)$ and a slope of $(1 + \delta_0)E/v$. Then the axial dispersion coefficient, E, and the intraparticle effective diffusivity, D_e, can be calculated.

The mass transport properties calculated for SG-3 are given in Table 4. The binary molecular diffusivity D_{AB}, was estimated by the method of Takahashi (32). The Peclet number, $Pe = 2vR/E$, was calculated from the axial dispersion coefficient and ranged from 0.013 to 0.257. The Peclet numbers obtained by Erkey and Akgerman (6) ranged from 0.058 to 0.244 for the naphthalene/alumina/SC-CO_2 system at temperatures of 298–318 K and pressures of 7.8–31 MPa and were in good agreement with those in this work. The ratio D_e/D_{AB}, which was expected to be less than unity due to the tortuosity, ranged from 0.002 to 0.716. The D_e/D_{AB} ratios were different for the two components, probably because of the difference of the structure of these two components: limonene is a ring compound and linalool is a linear compound. Since nonideal complex phenomena underlie the effective diffusivity in a simple adsorption/pore diffusion model, the D_e/D_{AB} value does not always agree for different components. The temperature or pressure dependency of the intraparticle effective diffusivities and the Peclet numbers were not observed due to scatter in the experimental data obtained by second moment analysis.

The contribution of each rate process to the second central moment was evaluated by using estimated parameters. Figure 8 shows the relative contribution of axial dispersion resistance, external mass transfer resistance, and intraparticle diffusion resistance as a function of the Reynolds number at 323 K and 14.7 MPa. The contribution of axial dispersion decreases with an increase in Re for both systems, while the intraparticle diffusion resistance becomes more important. The contribution of the external mass transfer resistance was less than 10% of all rate processes in both systems. This means that the effect of the estimation error of k_f is small enough for the calculation of the intraparticle effective diffusivity, especially at higher flow rates.

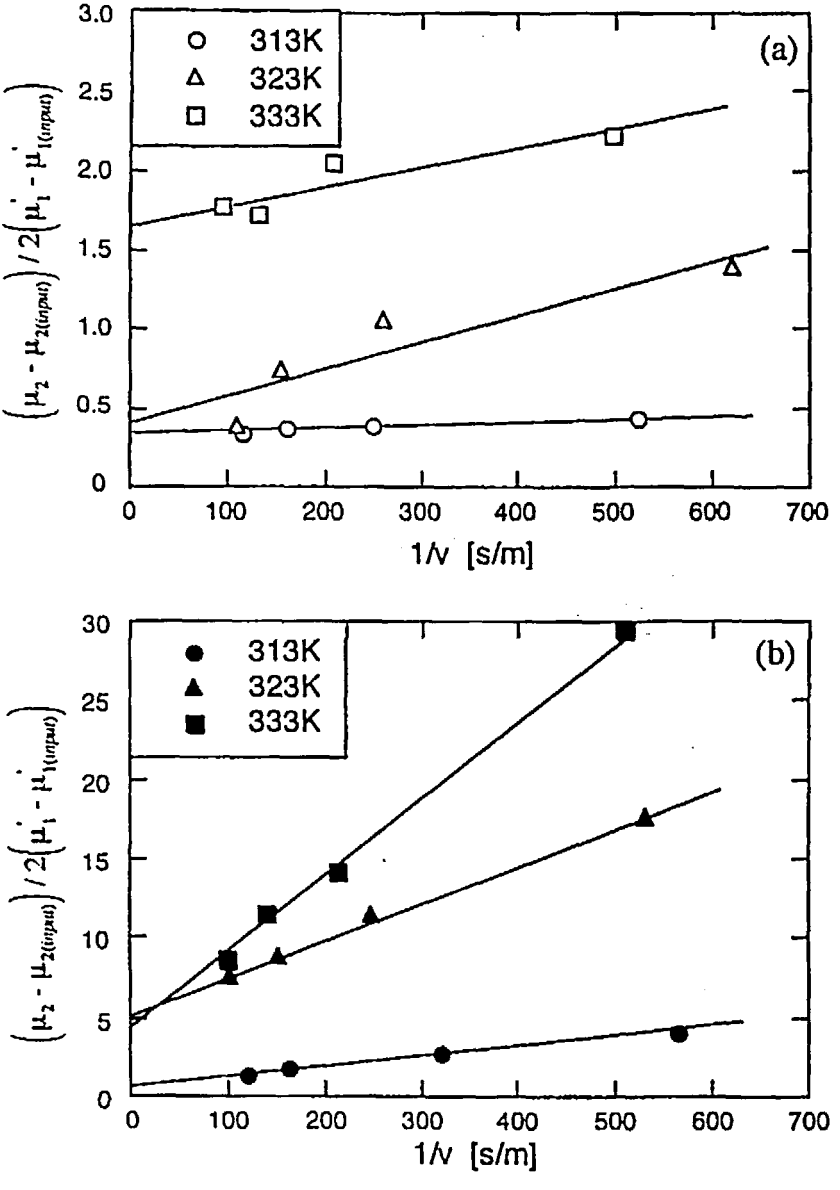

FIG. 7 Variation of the second moment with $1/v$ for the adsorption column at 14.7 MPa for SG-3: (a) limonene, (b) linalool.

TABLE 4
Mass Transport Parameters

Conditions			Limonene			Linalool		
Temperature (K)	Pressure (MPa)	$\eta \times 10^6$ (Pa·s)	$D_{AB} \times 10^9$ (m^2/s)	D_e/D_{AB} (—)	Pe (—)	$D_{AB} \times 10^9$ (m^2/s)	D_e/D_{AB} (—)	Pe (—)
313	11.8	52.4	16.0	0.016	0.462	14.0	0.121	0.157
313	14.7	62.9	9.7	0.017	0.085	9.0	0.600	0.537
313	17.7	69.9	7.8	0.010	0.063	7.2	0.099	0.081
313	23.5	80.1	5.4	0.018	0.365	5.0	0.106	0.398
323	11.8	36.1	19.0	0.022	0.153	17.0	0.607	0.184
323	14.7	50.2	13.0	0.013	0.013	12.0	0.040	0.181
323	17.7	59.2	9.8	0.003	0.103	9.2	0.288	0.108
323	23.5	71.1	6.9	0.019	0.257	6.4	0.422	0.210
333	11.8	28.5	23.0	0.036	0.117	21.0	0.716	0.141
333	14.7	39.2	17.0	0.003	0.206	15.0	0.054	0.125
333	17.7	49.0	13.0	0.002	0.155	12.0	0.023	0.045
333	23.5	62.6	9.3	0.128	0.019	8.7	0.124	0.155

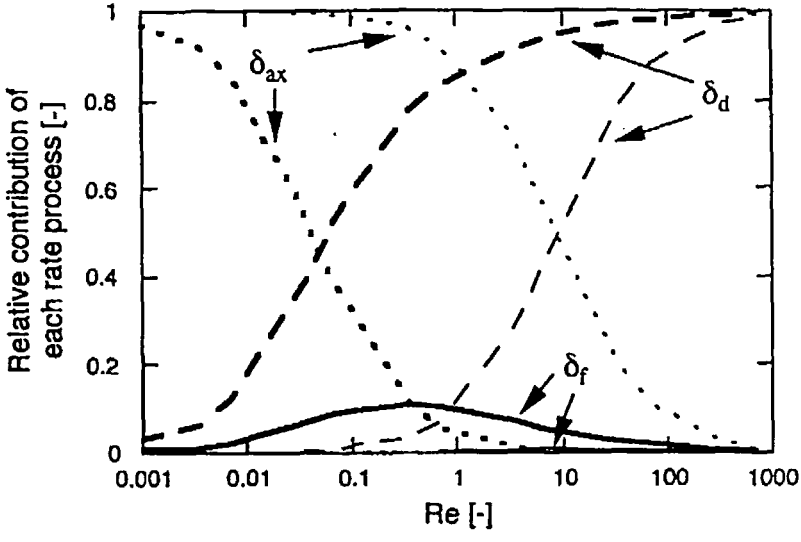

FIG. 8 Contribution of each rate process to peak broadening at 323 K and 14.7 MPa. Thin lines: limonene/silica gel/SC-CO_2 system. Thick lines: linalool/silica gel/SC-CO_2 system.

The evaluation of mass transport parameters from the second central moment is usually more difficult than the evaluation of equilibrium properties from the first moment because of a larger error in the calculation of second central moment. Furthermore, since the two-column system was used to avoid the effect of injection nonideality, the moment calculated has an even larger error. The values calculated for effective diffusivity and axial dispersion may be less accurate. Although the response measurement with a single column may give an analysis with less error than for the two-column system, the nonideality at the injector port, including slow dissolving of solute into the fluid, and the unknown shape of the impulse cannot be neglected. An injection system with the solute previously dissolved in a bulk fluid may give more reliable chromatographic analysis in the presence of a supercritical fluid.

CONCLUSIONS

The impulse response method of chromatographic analysis has been applied for limonene/silica gel/SC-CO_2 and linalool/silica gel/SC-CO_2 systems. In order to avoid the effect of nonideal behavior at sample injection, a two-column system, one for dissolving solute and one for adsorption, was used in this study. The importance of the two-column system was discussed by comparing results with a normal one-column system. By introducing a pre-column for dissolving solute into the system, the pure phenomena for supercritical fluid/solid system can be evaluated.

The adsorption equilibrium constant was evaluated by analyzing the first moment of the response curve. Linalool was more selectively adsorbed on silica gel than limonene. The adsorption equilibrium constant increased with an increase in temperature or a decrease in pressure.

The retrograde phenomenon in the vicinity of the critical point, compared with those in gas and liquid, was explained by strong interaction between solute and supercritical fluid, which was indicated by the apparent heat of adsorption and the large negative partial molar volume of solute. The apparent heat of adsorption was calculated from a van't Hoff plot. It indicated that the physical properties of a supercritical fluid approaches the liquid properties with an increase in pressure.

The intraparticle effective diffusivity and the Peclet number were calculated by analyzing the second central moment of the response curve, where the external film mass transfer coefficient was estimated by the Wakao–Kaguei correlation. The intraparticle effective diffusivity for linalool was larger than that of limonene. Temperature or pressure dependency of the intraparticle effective diffusivity and the Peclet number were not obvious because of a large error in the calculation of the second central moment. However, the orders of magnitude of the parameters were in good agreement with those

obtained for other supercritical fluid systems in the literature. Mass transport properties show that the contribution of axial dispersion resistance on broadening of the chromatographic response peak decreases with an increase in the Reynolds number, resulting from the relative importance of intraparticle diffusion resistance.

NOME

C	concentration (kg/m^3)
E	axial dispersion coefficient (m^2/s)
D_{AB}	molecular diffusivity (m^2/s)
D_e	intraparticle effective diffusivity (m^2/s)
ΔH_{app}	apparent heat of adsorption (kJ/mol)
h_i^0	enthalpy of solute for ideal gas (kJ/mol)
h_i^m	partial molar enthalpy of solute in mobile phase (kJ/mol)
h_i^s	partial molar enthalpy of solute on adsorbent (kJ/mol)
k	capacity factor (—)
K_A	adsorption equilibrium constant (—)
k_a	adsorption rate constant (1/s)
k_f	external mass transfer coefficient (m/s)
K_T	isothermal compressibility (1/Pa)
Pe	Peclet number, $2Rv/E$ (—)
R	particle radius (m)
R_g	gas constant (J/K·mol)
Re	Reynolds number, $2Rvr/h$ (—)
T	temperature (K)
t	time (s)
v	interstitial fluid velocity (m/s)
$V_i^{m\infty}$	partial molar volume of solute (m^3/mol)
Z	bed length (m)

Greek Symbols

α_m	volume expansivity (1/K)
ϵ	bed void fraction (—)
ϵ_p	particle voidage (—)
η	viscosity (Pa·s)
μ_1'	first absolute moment (s)
μ_2	second central moment (s^2)
ρ	fluid density (kg/m^3)
ρ_p	particle density (kg/m^3)

ACKNOWLEDGMENTS

This work was partly supported by a Grant-in-Aid for Research Fellow (No. 2362) from the Japan Society for the Promotion fo Science. The authors are grateful to Miss A. Ishikawa for experimental assistance.

REFERENCES

1. C. S. Tan and D. C. Liou, *Ind. Eng. Chem. Res.*, *27*, 988–991 (1988).
2. C. S. Tan and D. C. Liou, *Ibid.*, *28*, 1222–1226 (1989).
3. C. S. Tan and D. C. Liou, *Ibid.*, *29*, 1412–1415 (1990).
4. F. Recasens, B. J. McCoy, and J. M. Smith, *AIChE J.*, *35*, 951–959 (1989).
5. M. P. Srinivasan, J. M. Smith, and B. J. McCoy, *Chem. Eng. Sci.*, *45*, 1885–1895 (1990).
6. C. Erkey and A. Akgerman, *AIChE J.*, *36*, 1715–1721 (1990).
7. C. H. Lee and G. D. Holder, *Ind. Eng. Chem. Res.*, *34*, 906–914 (1995).
8. C. H. Lee, S. H. Byeon, and G. D. Holder, *J. Chem. Eng. Jpn.*, *29*, 683–694 (1996).
9. M. Goto, M. Sato, S. Kawajiri, and T. Hirose, *Sep. Sci. Technol.*, *31*, 1649–1661 (1996).
10. Y. Iwai, H. Uchida, Y. Mori, H. Higashi, T. Matsuki, T. Furuya, and Y. Arai, *Ind. Eng. Chem. Res.*, *33*, 2157–2160 (1994).
11. G. Madras, C. Erkey, and A. Akgerman, *Ibid.*, *32*, 1163–1168 (1993).
12. S. J. Macnaughton and N. R. Foster, *Ibid.*, *34*, 275–282 (1995).
13. S. Coppella and P. Barton, *ACS Symp. Ser.*, *329*, 201–212 (1987).
14. E. Stahl and D. Gerard, *Perfumer Flavorist*, *10*, 29–37 (1985).
15. Y. Yamauchi and M. Saito, *J. Chromatogr.*, *505*, 237–246 (1990).
16. F. Temelli, C. S. Chen, and R. J. Braddock, *Food Technol.*, *42*, 145–150 (1988).
17. D. Barth, D. Chouchi, G. D. Porta, and E. Reverchon, *J. Supercrit. Fluids*, *7*, 177–183 (1994).
18. D. Chouchi, D. Barth, and R. M. Nicoud, *Proc. 3rd Int. Symp. Supercrit. Fluids*, *2*, 183–188 (1994).
19. M. Kubin, *Collect. Czech. Chem. Commun.*, *30*, 1104–1118 (1965).
20. M. Suzuki, *Adsorption Engineering*, Kodansha and Elsevier, Tokyo, 1990.
21. D. M. Ruthven, *Principles of Adsorption and Adsorption Processes*, Wiley, New York, NY, 1984.
22. N. Wakao and S. Kaguei, *Heat and Mass Transfer in Packed Beds*, Gordon & Breach, New York, NY, 1985.
23. E. H. Chimowitz and F. D. Kelley, *J. Supercrit. Fluids*, *2*, 106–110 (1989).
24. F. D. Kelley and E. H. Chimowitz, *AIChE J.*, *36*, 1163–1175 (1990).
25. J.-J. Shim and K. P. Johnston, *J. Phys. Chem.*, *95*, 353–360 (1991).
26. P. G. Debenedetti, *Chem. Eng. Sci.*, *42*, 2203 (1987).
27. C. R. Yonker, R. W. Wright, S. L. Frye, and R. D. Smith, *ACS Symp. Ser.*, *329*, 172–188 (1987).
28. S. K. Kumar and K. P. Johnston, *J. Supercrit. Fluids*, *1*, 15 (1988).
29. D.-Y. Peng and D. B. Robinson, *Ind. Eng. Chem., Fundam.*, *15*, 59–64 (1976).
30. IUPAC, in *International Thermodynamic Tables of the Fluid State Carbon Dioxide* (S. Angus, B. Armstrong, and K. M. de Reuck, Eds.), Pergamon Press, New York, NY, 1976.
31. M. P. Srinivasan and B. J. McCoy, *J. Supercrit. Fluids*, *4*, 69–71 (1991).
32. R. C. Reid, J. M. Prausnitz, and B. E. Poling, *The Properties of Gases & Liquids*, 4th ed., McGraw-Hill, New York, NY, 1987.

Received by editor July 16, 1997
Revision received November 1997